

Polysiloxane-shield nano-patterned nanolayers: multi-component nano-reactors for photocatalytic purification

Roya Dastjerdi, Shiva Bahrizadeh

Textile Engineering Department, Yazd University, Yazd, Iran

*Corresponding author e-mail address: nanobiotex@yahoo.com; nanobiotex.dastjerdi@yazd.ac.ir

ABSTRACT

The efficiency of novel polysiloxane-shield nanolayers patterned by nanoparticles as durable bioactive-photocatalyst purifiers has been investigated in this paper. The effects of nanolayer surface modification, cross-linkable polysiloxane (XPs) treatment as well as pre-treatment of substrata on the photocatalyst activity of purifiers have been investigated in a variety of pHs. According to the results, interactions, surface patterning and orientations of nanostructures on the surfaces, controlled by the surface properties of applied nanostructures, played an effective role on the photodegradation efficiency. Results also revealed that polysiloxane shield nano-reactors, made through entrapping pollutant between nanoparticles and intercalated nanolayers sheltered by XPs, has also improved the efficiency via more effective impact on the entrapped molecules into the designed nano-reactors on the surfaces. As the results disclosed, the efficiency of nanoreactors was also directed by surface properties of nanostructures, their interactions and orientations. It was deduced that the best photodegradation efficiency was determined by providing the most electrostatic interactions between nanostructures and dye molecules, as the pollutants, at pH value of five.

Keywords: Bio-purification-like; bioactive multicomponent purifiers; polysiloxane shield nano-reactors; electrostatic interactions.

1. INTRODUCTION

Simultaneous control of microbial pollutions along with photodegradation of organic pollutants by photocatalyst nanostructures has sparked enormous interest in the field of bioactive purifiers [1-18]. In fact, the especial undoubted advantages bring up this method as a unique alternative for absorbent-based purifiers with at least three major advantages. The first one, is no need to subsequent procedures to extract the purified water as well as recover the adsorbents. The second, is simultaneous control of microbial pollution during purification process, and the third is that all pollutants degrade ultimately to naturally bio-purification-like products; H₂O and CO₂, which can be used to photosynthesis of green plants. Therefore, this process

is completely environmental friendly process. In fact, this purifiers direct a natural-like mechanism similar to unique naturally bio-purification and recycling of pollutants recovering them to the environment cycles. Therefore, designing the new purifiers on this basis and investigating their efficiency to achieve the optimized modifications would be an interesting demanding topic for research. Designing the multi-component nanocomposites [19-27] can be considered to accomplish the possible synergistic effects [28]. Here, novel multicomponent nanofunctionalization of nanoparticle-containing intercalated nanolayers were designed to develop treatments including nanostructures with different isotropic and anisotropic geometries.

2. EXPERIMENTAL SECTION

2.1. Materials. TiO₂ P25 supplied by Evonik Corporation has been used as the photocatalyst isotropic nanostructure. This commercial product contains 80wt% anatase and 20wt% rutile structures with 25–30 nm particle size [29]. Two type of modified and unmodified nano layers have been used as the anisotropic nanostructures including natural montmorillonite, Cloisite® Na+ and organo-modified montmorillonite (Cloisite® 30B: sodium

montmorillonite modified by methyl, tallow, bis-2-hydroxyethyl, quaternary ammonium chloride), produced by Southern Clay Company. Polysiloxane CT 208 E emulsion was kindly gifted by Wacker Finish.

2.2. Methods. The sample has been produced according to the method reported in our prior research [29], briefly as follows.

Table 1. Introducing of different samples [29].

Sample code	pre-treatment mercerizing	nano-layer functionalization		nanoparticle functionalization TiO ₂ NPs
		natural NLs	organo-modified NLs	
C	×	×	×	×
M.C	✓	×	×	×
NL	×	✓	×	×
ONL	×	×	✓	×
M.NL	✓	✓	×	×
M.ONL	✓	×	✓	×
NP	×	×	×	✓

Sample code	pre-treatment	nano-layer functionalization		nanoparticle functionalization
	mercerizing	natural NLs	organo-modified NLs	TiO ₂ NPs
M.NP	✓	✗	✗	✓
NL/NP	✗	✓	✗	✓
ONL/NP	✗	✗	✓	✓
M.NL/NP	✓	✓	✗	✓
M.ONL/NP	✓	✗	✓	✓

Colloidal solutions of 0.1wt% natural or organo-modified clay nano-layers (NLs or ONLs) have been prepared using magnetic stirrer and ultrasonic waves. Then, keeping the dispersing powers, the TiO₂ nanoparticles (NPs, 0.1wt%) have been gradually added to the clay colloidal solutions. The mercerized and unmercerized cotton fabrics have been treated via exhaustion process under ultrasonic waves for 45 min. The produced samples have been coded by their treatment components as NL, ONL, NP, NL/NP and ONL/NP (Table 1). For after-treatment by XPs, each sample was immersed in 2 wt% polysiloxane solution for 5 s and squeezed by pad to 100% wet pick-up and dried at 100 °C [29].

2.3. Characterization. The dye photodegradation process has been performed similar to our previous research [28] following Böttcher et al. [30], using Levafix Brill Rot Red 158 produced by

Dystar as a reactive dye ($\lambda_{max}=510$ nm) in a variety of pH (3-7) adjust by proper buffer solution of acetic acid and sodium acetate (for pH 3 and 5). The absorption intensities of dye effluents have been recorded by time applying a UV mini-1240 uv-vis spectrophotometer, Shimadzu, USA. A sample of dye solution without any fabric sample, termed Cb, has been considered in each process to identify the behavior of dye solution under the UV irradiation. The reflectance of filter samples used in dye decolorization process have been studied by an X-rite Spectrophotometer to distinguish if the dye molecules were absorbed by the filter, or really degraded through photocatalytic activity of TiO₂ NPS. The color differences of each sample before and after using in the purification process has been calculated and reported as ΔE along with the “L”, “a” and “b” as the values of Lightness, redness–greenness, yellowness–blueness, respectively.

3. RESULTS AND DISCUSSIONS

3.1. Photodegradation process at pH value of 5. A highly photo-stable dye molecule has been used to provide the test dye effluent. The data recorded in Table 2 also show that the dye decolorization cannot happen by UV irradiation without the photocatalytic activity of nanostructures in the blank sample (Cb). Increasing the absorption intensity in the blank sample by UV irradiation time may be associated with a UV-intensified resonance excitation phenomenon or forming some new complex under UV irradiation in water. However, only UV irradiation did not result in the dye decolorization. The results showed that the dye decolorization efficiency of pretreated (mercerized samples) functionalized by nano TiO₂ (M.NP) was more than that of unmercerized ones (compare Figures 1a & b). The data recorded in This is associated with absorption of more TiO₂ on the pretreated samples, as discussed in our fundamental investigations [29]. As shown in Figure 1a-d the dye decolorization efficiency of nano TiO₂ treated samples (M.NP and NP) was more than clay treated samples (M.NL, M.ONL, NL, ONL). Moreover, adding nano-clay to nano-TiO₂ not only did not improve the decolorization efficiency of TiO₂ but also decrease it via blocking the photon resulting in reducing the photocatalytic activity of TiO₂ (Figure 1a & b).

As shown in Figure 1a the best efficiencies have been recorded by using mercerized TiO₂ treated sample (M.NP) as well as mercerized organo-modified montmorillonite and TiO₂ treated sample (M.ONL/NP). The efficiency of mercerized organo-modified montmorillonite and TiO₂ (M.ONL/NP) was more than mercerized natural montmorillonite and TiO₂ (M. NL/NP). By using these samples about 87% and 79% decolorization efficiency

have been recorded after 1.5 h and the complete decolorization have been recorded after 2.5 h and 3 h, respectively.

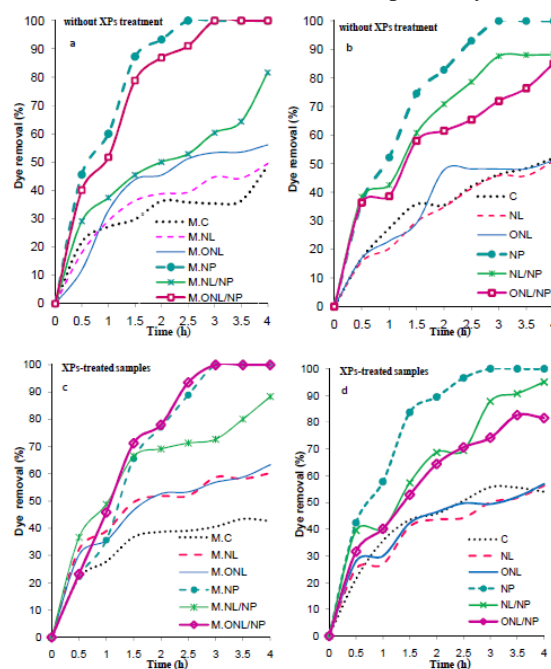


Figure 1. Photocatalytic dye decolorization efficiencies at pH=5.

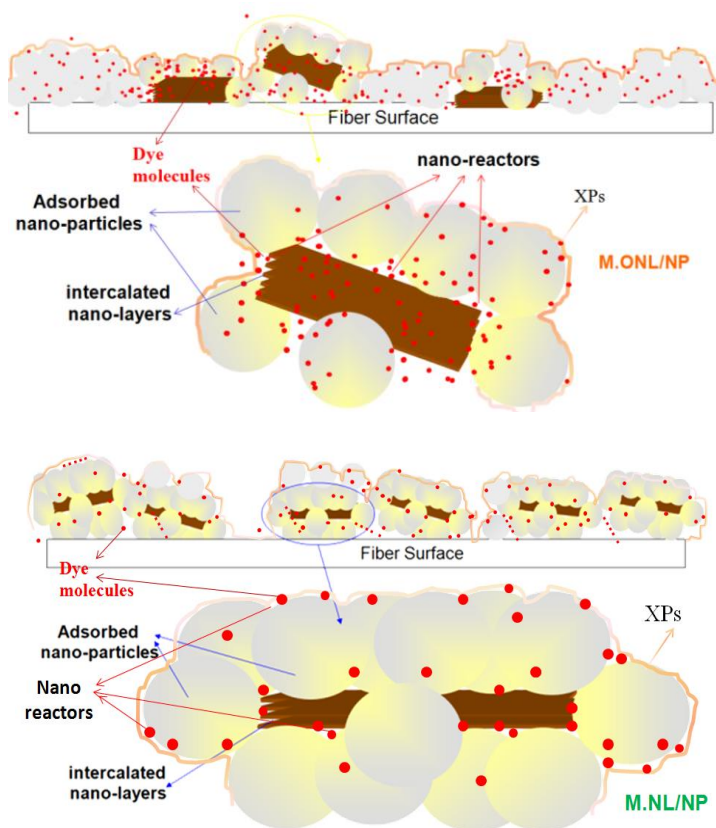
Table 2. Absorption intensities of blank sample (Cb).

Time (h)	pH=3	pH=5
	Absorption intensity	Absorption intensity
0	17.15	17.16
0.5	22.03	17.58
1	22.08	16.07

Time (h)	pH=3	pH=5
	Absorption intensity	Absorption intensity
1.5	22.2	17.71
2	22.22	19.07
2.5	23.19	19.02
3	23.37	19.63
3.5	23.56	19.73
4	23.96	21.51

This is in full-agreement with the raised hypothesis in our earlier study [29] in the case of the less co-covering of NPs and nanolayers on the sample treated with organo-modified montmorillonite and TiO₂ due to their surface charges and differences of their surface energies.

As it has been discussed, co-covering of NPs by nanolayers can limit receiving the photon to NPs and reduce the photocatalytic activity of TiO₂ NPs. The spectrophotometric studies of filters after the decolorization process proved the dye degradation during decolorization process upon using the best samples. L0, a0 and b0 associated with the samples before using in the decolorization process have been taken to calculate ΔE (Table 3). Then, higher value of ΔE shows dye absorption while decreasing ΔE along with good decolorization efficiency shows the desirable dye degradation through the dye decolorization process.



Scheme 1. Polysiloxane-shield nano-patterned nanolayers as multi-component nano-reactors for photocatalytic purification reproduced from the preceding research [29] and adapted for demonstrating the dye degradation nano-reactors.

For instance, high value of ΔE near to untreated sample recorded for sample functionalized with only clay shows that the mechanism of decolorization in the case of these samples is dye

absorption but not the dye degradation, because clay does not demonstrate photocatalytic activity. However, negligible ΔE (Table 3) on mercerized samples functionalized by TiO₂ (M.NP) as well as mercerized organo-modified montmorillonite and TiO₂ (M.ONL/NP) as the best sample proved the real dye photodegradation via photocatalyst activity of TiO₂ NPS.

The results recorded by XPS-treated mercerized samples (Figure 1c) demonstrated also the same effect. The samples functionalized by TiO₂ (M.NP) as well as organo-modified montmorillonite and TiO₂ (M.ONL/NP) showed the best efficiency. However, the enhanced efficiency of un-mercerized XPs-treated TiO₂ functionalized samples (NP) as compared to that of mercerized one (M.NP) can be associated to super hydrophobicity of the mercerized sample which delays the dye adsorption in the beginning. However, as dye adsorption takes place, the dye degradation will follow faster due to presence of more TiO₂ NPs on the surface to some extent. The spectrophotometric studies of filters after the decolorization process (Table 3) proved the dye degradation during decolorization process upon using the best samples. After XPS-treatment the efficiency of TiO₂/clay functionalized sample (especially M.ONL/NP) has been enhanced and reach to TiO₂-functionalized sample or even more. This implies the mechanism raised in our previous research [28] in the case of accelerated degradation of entrapped dye molecules into the polysiloxane-shield nano-reactors. In fact, active oxygen species, generated by TiO₂, were significantly blocked between the XPs-shield intercalated nanolayers and can drastically impact the entrapped dye molecules. In this way, the dye molecules are in close contact with concentrated active oxygen species into the created nano-reactors (scheme 1) providing an accelerated degradation of dye molecules. Consequently, the XPs coating can compensate for the decrease of the photo-blocking effect of nanolayers. Evaluation of the antibacterial efficiency of samples proved an excellent photo-bioactivity [29] in the case of samples with the best photocatalytic dye decolorization efficiencies reported in this paper.

3.2. Photodegradation process at pH value of 3. The similar results have been obtained upon using pH=3. Similarly, the samples functionalized by TiO₂ (M.NP) as well as organo-modified montmorillonite and TiO₂ (M.ONL/NP) showed the best efficiency (Figure 2). It should be pointed out that, in this condition, the efficiency of sample functionalized by natural montmorillonite, Cloisite® Na⁺ and TiO₂ has also reached the efficiency of organo-modified montmorillonite and TiO₂.

This can be related to the increase of positive surface charge of Na⁺ on the natural montmorillonite by decreasing the pH, providing more affinity to adsorb the dye molecules, especially on the XPs-treated sample which adsorbed dye molecules are in close contact with concentrated active oxygen species into the created nano-reactors. However, the efficiency of dye degradation at pH=5 is more than pH=3. As it has been discussed before [28], the absorbed dye molecules on the surface can be degraded faster in near contact to more concentrated of active oxygen species generated by the photocatalyst activity of TiO₂ NPs. The point of zero charge for TiO₂ has been recorded at a pH of 5.6 [31]. Then, it is expected that by decreasing the pH value from 5 to 3 the positive surface charge of NPs and consequently their affinity to absorb dye molecules would be

increased. However, the contradictory effect showed that some negative groups of dye molecules may be protonated in low pH. This reduced their negative surface charges dominating the effect of increasing positive surface charges of NPs.

3.3. Photodegradation process at pH value of 7. The results (Figure 3) showed a similar trend to pH=3 and 5, however, with the decreased efficiency. Considering the point of zero charge for TiO₂ (pH = 5.6) [31], the TiO₂ nanoparticles have been negatively charged at pH = 7 [32, 33].

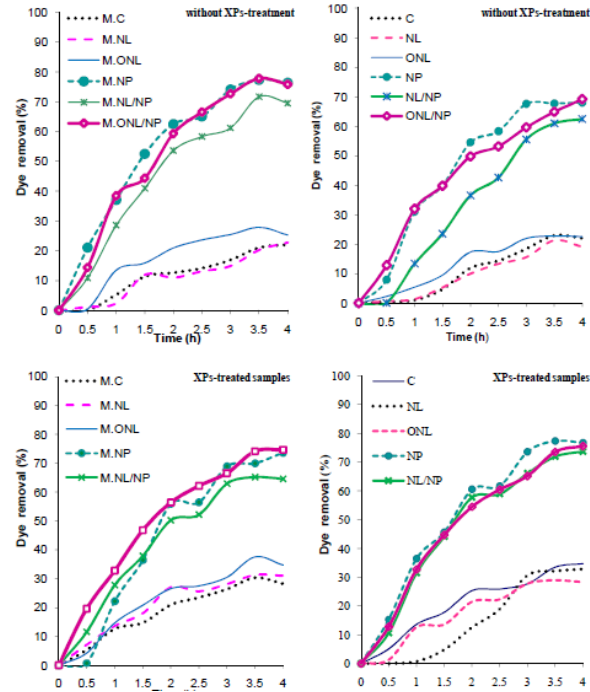


Figure 2. Photocatalytic dye decolorization efficiencies at pH=3.

This reduced the affinity of dye molecules with anionic groups to adsorb on the samples. Although the density of positive surface charge on clay nanolayers has been also reduced at this

pH, natural montmorillonite, Cloisite® Na⁺ has the relatively most positive surface charge density.

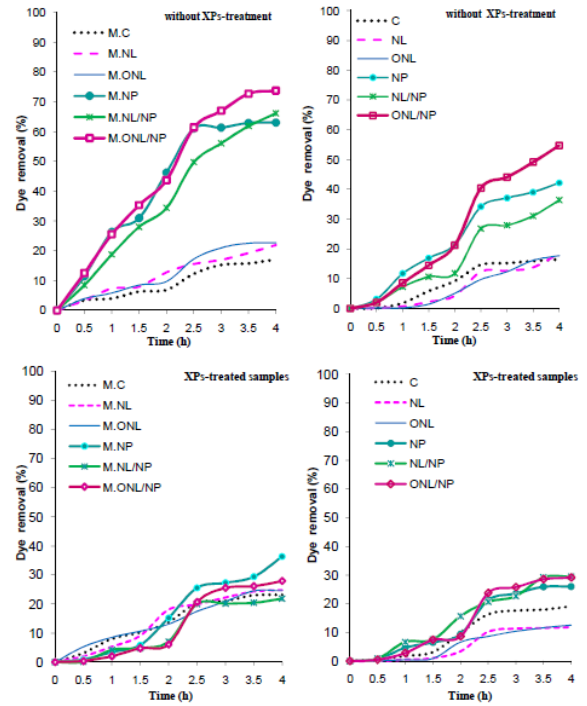


Figure 3. Photocatalytic dye decolorization efficiencies at pH=7.

The results also show, the efficiency of sample functionalized by natural montmorillonite and TiO₂ (NL/NP) has been reached to the best samples proving the efficiency of the surface charge and dye adsorption. However, the overall decolorization efficiency of samples has been reduced in this condition. Consequently, the best condition was determined by providing the highest affinity of dye adsorption passing of an optimum of pH=5.

Table 3. The color differences of each sample before and after using in the purification process.

pH	Samples	Without XPs				XPs-treated			
		L	a	b	ΔE	L	a	b	ΔE
5	MC	77.07	22.52	-4.44	26.71	75.46	23.99	-4.09	28.63
	C	79.65	18.69	-3.28	21.98	77.62	20.77	-3.08	24.64
	M.NL	79.93	21.87	-3.91	26.09	76.16	22.51	-3.2	26.85
	NL	78.79	19.68	-2.88	23.13	78.82	19.06	-2.1	22.4
	M.ONL	76.83	21.97	-3.59	26.16	76.27	21.9	-3.02	26.24
	ONL	79.05	20.05	-2.94	23.34	77.41	21.95	2.73	25.68
	M.NP	86.64	4.27	0.00	5.73	83.67	10.45	2.32-	12.96
	NP	84.91	9.57	-1.34	11.37	86.22	6.96	0.24	8.12
	M.NL/NP	79.38	16.45	-4	20.67	80.78	15.07	-2.72	18.24
	NL/NP	82.78	12.79	-2.52	15.53	82.12	14.2	-2.44	16.82
3	M.ONL/NP	86.08	5.52	-0.45	7.16	85.76	7.47	-0.56	8.98
	ONL/NP	81.58	15.48	-2.93	18.29	82.08	16.27	-3.13	18.84
	MC	77.66	21.25	-3.97	25.24	75.74	21.68	-3.44	26.41
	C	79.82	18.42	-3.13	21.64	78.75	19.31	-3.47	22.86
	M.NL	77.25	21.31	-3.68	25.41	76.37	21.83	-3.34	26.2
	NL	79.19	19.83	-3.00	23.1	78.96	18.20	-1.94	21.57
	M.ONL	76.82	22.55	-3.59	26.65	76.64	21.81	3.21-	26.02
	ONL	78.98	20.13	-2.97	23.45	77.21	22.16	-3.21	26.05
	M.NP	86.22	5.99	-1.09	7.76	84.35	9.82	-1.81	11.96
	NP	84.35	11.2	-2.18	13.27	85.61	8.90	-0.66	10.31

pH	Samples	Without XPs				XPs-treated			
		L	a	b	ΔE	L	a	b	ΔE
7	M.NL/NP	84.3	8.35	-1.09	10.51	81.83	13.03	-2.14	15.87
	NL/NP	83.83	12.61	-2.46	14.77	84.17	10.10	-0.57	11.91
	M.ONL/NP	85.88	6.16	-0.77	7.90	84.87	8.65	-1.05	10.5
	ONL/NP	84.39	9.90	1.45	11.9	85.35	11.05	-1.31	12.52
	MC	80	10.65	-2.03	13.26	79.54	10.87	-1.48	13.77
	C	82.49	8.32	-0.85	9.89	81.47	8.46	0.42	10.36
	M.NL	80.03	10.63	-1.98	13.21	79.66	10.62	-1.41	13.49
	NL	82.71	8.25	-0.68	9.69	82.41	7.53	0.50	9.09
	M.ONL	80.08	10.47	-2.08	13.09	80.03	11.01	-1.59	13.67
	ONL	82.82	8.45	-0.96	9.94	82.29	8.45	-0.57	10.18
	M.NP	82.79	4.38	-0.43	6.45	82.41	9.33	-1.92	11.31
	NP	84.29	6.39	-1.23	7.97	84.18	7.79	-1.32	9.16
	M.NL/NP	82.70	6.27	-0.47	7.95	81.16	9.41	-1.13	11.67
	NL/NP	83.86	7.46	-1.10	8.88	83.84	7.59	-1.44	9.13
	M.ONL/NP	84.35	4.58	-0.53	6.12	83.78	5.74	-0.55	7.25
	ONL/NP	84.75	5.80	-1.13	7.36	84.76	7.50	-1.66	8.90

4. CONCLUSIONS

The similar trends for the different treatments have been obtained upon using various pH of 3, 5 and 7. Similarly, the mercerized samples functionalized by TiO₂ (NP) as well as organo-modified montmorillonite and TiO₂ (NL/NP) showed the best dye degradation efficiency along with the excellent bioactivity. The absorbed dye molecules on the surface can be degraded faster in near contact to more concentrated of active oxygen species generated by the photocatalyst activity of TiO₂ NPs. Consequently, the best condition determined by providing the highest affinity of dye adsorption passing of an optimum of pH=5. At pH=3 some negative groups of dye molecules can be protonated in low pH. This reduced their negative surface charges as well as their affinity. Considering the point of zero charge for TiO₂ (pH=5.3) [31], the TiO₂ nanoparticles have been negatively charged at pH=7. This reduced the affinity of dye molecules with anionic groups to adsorb on the samples. Consequently, the optimum accomplished upon using pH=5. The dye degradation

efficiency of nano-TiO₂ treated samples was more than clay treated samples. The positive effect of the pretreatment (mercerizing) has been revealed. The efficiency of organo-modified montmorillonite and TiO₂ was more than that of natural montmorillonite and TiO₂. However, adding nano-clay to nano-TiO₂ not only did not improve the degradation efficiency but also decreased it by blocking the photon resulted in reducing the TiO₂ photocatalyst activity. After XPs-treatment, the efficiency of TiO₂/clay functionalized sample enhanced and reached to TiO₂-functionalized sample or even more. This implies the accelerated degradation of entrapped dye molecules into the polysiloxane-shield nano-reactors. In fact, active oxygen species generated by TiO₂ were significantly blocked between the XPs-shield intercalated nanolayers and can drastically impact on the entrapped dye molecules. All the results were in full-agreement with the hypotheses and models raised our preceding report [29].

5. REFERENCES

- [1] V.K. Gupta, R. Jain, A. Mittal, M. Mathur and S. Sikarwar, Photochemical degradation of the hazardous dye Safranin-T using TiO₂ catalyst, *J Colloid Interface Sci.*, 309, 464, **2007**.
- [2] G. Rajagopal, S. Maruthamuthu, S. Mohanan and N. Palaniswamy, Biocidal effects of photocatalytic semiconductor TiO₂, *Colloids Surf., B: Biointerfaces*, 51, 107, **2006**.
- [3] S. Subramanian and R. Seeram, Fabrication of Functionalized Nanofiber Membranes Containing Nanoparticles, *J. Nanosci. Nanotechnol.*, 10, 1139, **2010**.
- [4] Yoshitake Masuda, Makoto Bekki, Shuji Sonezaki, Tatsuki Ohji and Kazumi Kato, Dye Adsorption Characteristics of Anatase TiO₂ Film Prepared in an Aqueous Solution, *Thin Solid Films*, 518, 845, **2009**.
- [5] R. Dastjerdi and M. Montazer, A Review on the Application of Inorganic Nanostructured Materials in Modification of Textiles: Focus on Anti-microbial, *Colloids Surf., B: Biointerfaces*, 79, 5, **2010**.
- [6] S. Chakrabarti and B.K. Dutta, Photocatalytic degradation of model textile dyes in wastewater using ZnO as semiconductor catalyst, *J. Hazard. Mater.*, 112, 269, **2004**.
- [7] D. Gümüř and F. Akbal, Photocatalytic Degradation of Textile Dye and Wastewater, *Water Air Soil Pollut.*, 216, 117, **2011**.
- [8] S. Sundarajan, A. Venkatesan and S. Ramakrishna, Fabrication of Nanostructured Self-Detoxifying Nanofiber Membranes that Contain Active Polymeric Functional Groups, *Macromol. Rapid Commun.*, 30, 1769, **2009**.
- [9] Y. Zhang, Y. Fan, C. Sun, D. Shen, Y. Li and J. Li, Functionalized polydiacetyleneglycolipid vesicles interacted with Escherichia coli under the TiO₂ colloid, *Colloids Surf., B: Biointerfaces*, 40, 137, **2005**.
- [10] M. Muruganandham and M. Swaminathan, Solar photocatalytic degradation of a reactive azo dye in TiO₂-suspension, *Sol. Energy Mater. Sol. Cells*, 81, 439, **2004**.
- [11] P. Dhandapani, S. Maruthamuthu and G. Rajagopal, Bio-mediated synthesis of TiO₂ nanoparticles and its photocatalytic effect on aquatic biofilm, *Journal of photochemistry and*

- photobiology. *B, Biology, J. Photochem. Photobiol. B.*, 110, 43, **2012**.
- [12] M. Saquib, M. Abu Tariq, M.M. Haque and M. Muneer, Photocatalytic degradation of disperse blue 1 using UV/TiO₂/H₂O₂ process, *J. Environ. Manage.*, 88, 300, **2008**.
- [13] M. Teng, F. Li, B. Zhang, , A. A. Taha, Electrospun cyclodextrin-functionalized mesoporous polyvinyl alcohol/SiO₂ nanofiber membranes as a highly efficient adsorbent for indigo carmine dye, *Colloids Surf., A: Physicochem. Eng. Aspects*, 385, 229, **2011**.
- [14] P. Wongkalasin and S. Chavadej, Thammanoon Sreethawong, Photocatalytic degradation of mixed azo dyes in aqueous wastewater using mesoporous-assembled TiO₂ nanocrystal synthesized by a modified sol-gel process, *Colloids Surf., A: Physicochem. Eng. Aspects*, 384, 519, **2011**.
- [15] G. Zayani, L. Bousselmi, F. Mhenni, and A. Ghrabi, Solar photocatalytic degradation of commercial textile azo dyes: Performance of pilot plant scale thin film fixed-bed reactor, *Desalination*, 246, 344, **2009**.
- [16] F. Magalhães and R.M. Lago, Floating photocatalysts based on TiO₂ grafted on expanded polystyrene beads for the solar degradation of dyes, *Solar Energy*, 83, 1521, **2009**.
- [17] V. K. Gupta, R. Jain, S. Agarwal and M. Shrivastava, Kinetics of photo-catalytic degradation of hazardous dye Tropaeoline 000 using UV/TiO₂ in a UV reactor, *Colloids Surf., A: Physicochem. Eng. Aspects*, 378, 22, **2011**.
- [18] H. Xu, H. Li, G. Sun, J. Xia, C. Wu, Z. Ye and Q. Zhang, Photocatalytic activity of La₂O₃-modified silver vanadates catalyst for Rhodamine B dye degradation under visible light irradiation, *Chem. Eng. J.*, 160, 33, **2010**.
- [19] R. Dastjerdi, M. Montazer and S. Shahsavan, A novel technique for producing durable multifunctional textiles using nanocomposite coating, *Colloids Surf., B: Biointerfaces*, 81, 32, **2010**.
- [20] H. Zhang, X. Lv, Y. Li, D. Chen D, L. Li and J. Li, P25-Graphene Composite as a High Performance Photocatalyst, *ACS Nano*, 4, 380, **2010**.
- [21] H. J. Kima, M. K. Joshia, H. R. Panta, J. H. Kima, E. Lee, C. S. Kima, One-pot hydrothermal synthesis of multifunctional Ag/ZnO/fly ash nanocomposite, *Colloids Surf., A: Physicochem. Eng. Aspects*, 469, 256, **2015**.
- [22] R. Dastjerdi, M.R.M. Mojtahedi and A. M. Shoshtari, Investigating the Effect of Various Blend Ratios of Prepared Masterbatch Containing Ag/TiO₂ Nanocomposite on the Properties of Bioactive Continuous Filament Yarns, *Fibers Polym.*, 9, 727, **2008**.
- [23] X. Jiang, L. Yang, P. Liu, X. Li and J. Shen, The photocatalytic and antibacterial activities of neodymium and iodine doped TiO₂ nanoparticles, *Colloids Surf., B: Biointerfaces*, 79, 69, **2010**.
- [24] R. Dastjerdi and M. R. M. Mojtahedi, Multifunctional Melt-Mixed Ag/TiO₂ Nanocomposite PP Fabrics: Water Vapour permeability, UV Resistance, UV protection and Wear properties, *Fibers Polym.*, 14, 2, 298, **2013**.
- [25] J.A. Lee, K.C. Krogman, M. Ma, R. M. Hill, P.T. Hammond, and G.C. Rutledge, Highly Reactive Multilayer-Assembled TiO₂ Coating on Electrospun Polymer nanofibers, *Adv. Mater.*, 21, 1252, **2009**.
- [26] R. Dastjerdi, New Features of Silver/Zinc Loaded Nanocomposite Textiles; Dyeability, Abrasion Resistance and Comfort, *J. Eng. Fibers Fabr.*, 452, 25–31, **2014**.
- [27] S. Vivekanandhan, M. Schreiber, C. Mason, A.K. Mohanty and M. Misra, Maple leaf (*Acer* sp.) extract mediated green process for the functionalization of ZnO powders with silver nanoparticles, *Colloids Surf., B: Biointerfaces*, 113, 169, **2014**.
- [28] R. Dastjerdi, M. Montazer, S. Shahsavan, H. Bo'ttcher, M. B. Moghadam and J. Sarsour, Novel durable bio-photocatalyst purifiers, a non-heterogeneous mechanism: Accelerated entrapped dye degradation into structural polysiloxane-shield nano-reactors, *Colloids Surf., B: Biointerfaces*, 101, 457, **2013**.
- [29] R. Dastjerdi, A. Scherrieble, S. Bahrizadeh, F. A. Sadrabadi, L. Hedaya, A Key Major Guideline for Engineering Bioactive Multicomponent Nanofunctionalization for Biomedicine and Other Applications: Fundamental Models Confirmed by Both Direct and Indirect Evidence, Article ID 2867653, <https://doi.org/10.1155/2017/2867653>, **2017**.
- [30] H. Bo'ttcher, B. Mahltig, J. Sarsour, T and Stegmaier, Qualitative investigations of the photocatalytic dye destruction by TiO₂-coated polyester fabrics, *J Sol-Gel Sci Technol*, 55, 177, **2010**.
- [31] T.T.Y. Tan, C.K. Yip, D. Beydoun and R. Amal, Effects of nano-Ag particles loading on TiO₂ photocatalytic reduction of selenate ions, *Chem. Eng. J.*, 95, 179, **2003**.
- [32] R. Dastjerdi and M. Montazer, Nano-colloidal functionalization of textiles based on polysiloxane as a novel photo-catalyst assistant: processing design, *Colloids Surf., B: Biointerfaces*, 88, 381, **2011**.
- [33] R. Dastjerdi, M. Montazer, T. Stegmaier and M. B. Moghadam, A smart dynamic self-induced orientable multiple size nano-roughness with amphiphilic feature as a stainrepellent hydrophilic surface, *Colloids Surf., B: Biointerfaces*, 91, 280, **2012**.

ACKNOWLEDGEMENTS

Authors would also like to acknowledge the contributions of Evonik Corporation (Germany) and Wacker Finish (Germany) for kindly providing nano TiO₂ and polysiloxane emulsion, respectively.

© 2018 by the authors. This article is an open access article distributed under the terms and conditions of the Creative Commons Attribution license (<http://creativecommons.org/licenses/by/4.0/>).